

# Low-current hollow-cathode discharge in a trigger unit of a cold cathode thyatron

N V Landl<sup>1,2</sup>, Y D Korolev<sup>1,2,3</sup>, O B Frants<sup>1,2</sup>, V G Geyman<sup>1</sup>, A V Bolotov<sup>1</sup>

<sup>1</sup> Institute of High Current Electronics SB RAS, 634055 Tomsk, Russian Federation

<sup>2</sup> Tomsk State University, 634050 Tomsk, Russian Federation

<sup>3</sup> Tomsk Polytechnic University, 634050 Tomsk, Russian Federation

E-mail: landl@lnp.hcei.tsc.ru

**Abstract.** The paper deals with the investigations of the effect of cathode emissivity on the regimes of low-current hollow-cathode glow discharge. It is shown that an increase in the emissivity due to the so-called high-emissivity tablet allows the essential decrease in the discharge initiation voltage and the discharge burning voltage. The model of current sustaining for the hollow-cathode discharge, which takes into account the external emission current has been developed. On basis of the model, the current-voltage characteristics of the discharge have been interpreted.

## 1. Introduction

Since the end of 1980's, a considerable interest has been generated in a new type of low-pressure switching device with a cold cathode, often named the pseudospark switch or the cold cathode thyatron [1–8]. A range of operating pressures of the switch corresponds to the conditions of the left branch of Paschen's curve when the electron free path for ionization is much in excess of the electrode separation. Under such conditions, for both self-breakdown of the main gap of the switch and for external discharge triggering a considerable prebreakdown electron current is required [2–4]. This current is provided due to a trigger unit that is placed in the cathode cavity of the main gap [3].

Various types of the trigger units are used in the switches [1, 3]. One type of the trigger devices is based on an auxiliary low-current hollow-cathode glow discharge. The conditions of the auxiliary discharge burning significantly determine the rating characteristics of the switch itself. Therefore, the investigations of the auxiliary discharge seem to be of a great importance.

In this paper, the data on the influence of the cathode emissivity on the regimes of the auxiliary glow discharge are presented. The model for current sustaining in hollow-cathode discharge has been developed. The current-voltage characteristics are interpreted with a usage of the model.

## 2. Experimental setup and summary of experimental data

The experiments were carried out with the sealed-off switches TPI1-10k/50 [3] whose schematic arrangement is shown in figure 1. The ceramic casing of the device has an external diameter of 95 mm. The operating pressure is maintained due to a hydrogen reservoir that is powered by a voltage  $V_H$  at a current of about 2 A. The auxiliary glow discharge in the trigger unit is initiated and sustained due to the power supply  $V_1$ . The cathode cavity has the following dimensions: cavity diameter  $D = 3$  cm, cavity height  $h = 2.9$  cm. The cavity  $C_1$  communicates with the main cathode cavity  $C$  via the axial hole with a diameter  $D_1 = 1.2$  cm. Due to this hole a parasitic current  $i_2$  inevitably flows from the



anode  $A_1$  to the cathode cavity  $C$ . The presence of this parasitic current can lead to decreasing the breakdown voltage of the main gap. In the experiments we measured the separate components of the total discharge current  $i$ , as figure 1 shows ( $i = i_1 + i_2 + i_G$ ).

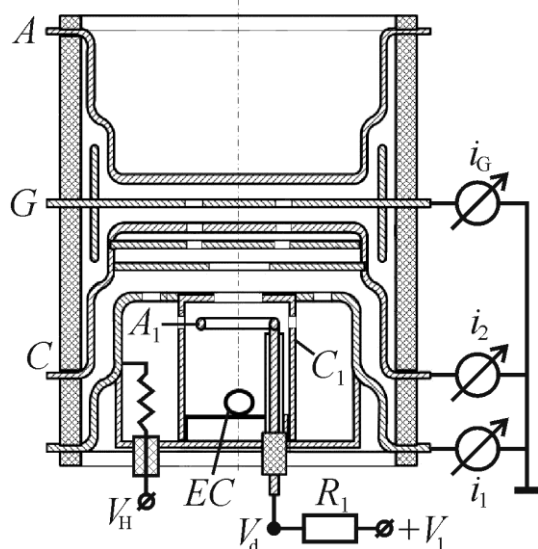


**Figure 1.** Schematic arrangement of the switch TPI1-10k/50 and the method of measurement of current-voltage characteristics.  $A$  – anode of the switch,  $C$  – hollow cathode of the switch,  $G$  – intermediate gradient electrode,  $A_1$  – ring anode of the auxiliary glow discharge,  $C_1$  – hollow cathode of the auxiliary glow discharge,  $EC$  – high emissivity cylinder,  $V_1$  – voltage for powering the auxiliary glow discharge,  $V_H$  – voltage for powering of a hydrogen reservoir,  $R_1 = (20 - 65)$  k $\Omega$  – ballast resistor.

To increase the cathode emissivity the so-called high-emissivity tablet (emissivity cylinder)  $EC$  is used. The tablet is placed in the hollow cathode  $C_1$ . It represents a hollow cylinder that is fabricated from the powder materials by means of hot-pressing and sinter technology [3]. The basic component of the cylinder is the powder tungsten (90 %) to which aluminium oxide and cesium carbonate are added. In experiments we also used the switches without high-emissivity without tablet.

As far as the experiments were carried out with the sealed-off switches, a gas pressure in the switch was determined by the hydrogen reservoir that was powered by a voltage  $V_H$ . Then from one switch to the other, the same gas pressure can be achieved at different values of  $V_H$ . Since the geometry of the main gap was identical, we estimated a gas pressure inside the switches by measuring the static breakdown voltage in the main gap.

Figure 2 shows a typical current-voltage characteristic of the auxiliary glow discharge and a fraction of parasitic current in total discharge current  $i_2/i$  for the switch without the high-emissivity cylinder. The characteristic is rather intricate. Discharge is able to burn in two regimes. Regime  $I$  corresponds to the so-called hampered glow discharge with hollow cathode. In this regime a length of the cathode voltage drop region is comparable with the radius of hollow cathode  $D/2$  and a negative glow region is not distinctly observed. In this regime, increasing of the voltage  $V_1$  shifts the operating point over the curve to the right. When we decrease a voltage of power supply  $V_1$ , then in a vicinity of point  $I$ , the discharge is extinguished.

A critical value of the discharge current corresponds to point 3 in the current-voltage characteristic. A further increase in voltage  $V_1$  leads to a sharp transition to the regime  $II$  (to point 4). In this mode of operation, the negative glow region appears. The discharge conditions are transformed from the hampered regime to an ordinary glow discharge with hollow cathode. In the regime  $II$  a hysteresis of current-voltage characteristic takes place. When we decrease a voltage  $V_1$ , the operating point is shifted to the left up to point 5. After that a reverse abrupt transition to the hampered regime  $I$  occurs.

The same characteristics with hysteresis are typical for a wide range of gas pressure (voltages  $V_H$ ). The main features of the discharge without high-emissivity tablet are rather high values of the discharge initiation voltage and of the discharge burning voltage  $V_d$ . For example, for  $V_H = 6.2$  V and  $V_H = 5.6$  V the discharge initiation voltages are 1230 V and 3500 V correspondently.

A current-voltage characteristic for the case of the enhance cathode emissivity is shown in figure 3. The principal difference from the conditions without tablet is the absence of the abrupt transition from regime  $I$  to regime  $II$ . The discharge burning voltage is essentially decreased (up to a value  $V_d \approx 130$

V). As for the discharge initiation voltage (the static breakdown voltage in the trigger unit), this value corresponds to 380 V for  $V_H = 5$  V and to 280 V for  $V_H = 5.6$  V.

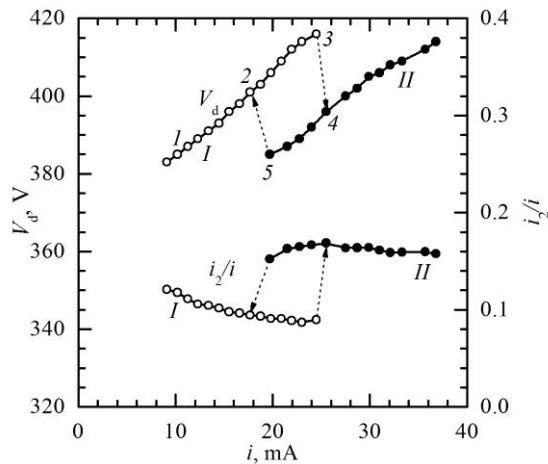


**Figure 2.** Current-voltage characteristic for the auxiliary glow discharge and a fraction of parasitic current in total discharge current  $i_2/i$  for the trigger unit without the emissivity cylinder.

$V_H = 6.2$  V,  $R_1 = 25.6$  k $\Omega$ .

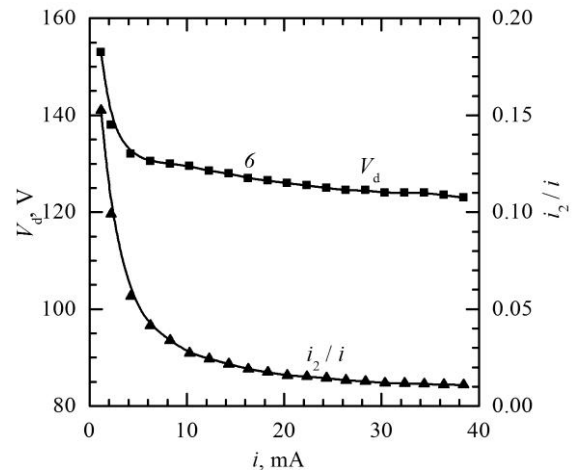


**Figure 3.** Current-voltage characteristics for the auxiliary glow discharge and a fraction of parasitic current in total discharge current  $i_2/i$  for the trigger with the emissivity cylinder.

$V_H = 5.6$  V,  $R_1 = 65$  k $\Omega$ .

As noted earlier, when the glow discharge burns between the electrodes  $A_1$  and  $C_1$ , some fraction of the current inevitably flows from the anode to the main cathode cavity  $C$ . In general, this current has to be minimized. For the cases of the cathode with the high emissivity a current to the electrode  $C$  does not exceed 4 % of the current  $i$  in wide range of the discharge current in the trigger unit, whereas for the cathode with an ordinary emissivity the fraction of current can achieve to 20 %.

### 3. Description of the model and interpretation of the experimental data

It is convenient to interpret the regimes of the auxiliary glow discharge and to carry out the corresponding estimations with a usage of the model that had been developed earlier for the high-current hollow-cathode pulsed glow discharge [5]. Illustration of the essence of this model is shown in figure 4. The cathode cavity  $C$  is filled with the negative glow plasma  $NG$ . The electrons emitted from the cathode are accelerated in the cathode layer  $l_c$  by the voltage drop  $V_c$  and the energy of the fast oscillating electron is spent for sustaining the negative glow plasma.

A steady state plasma density in the hollow cathode is established due to a balance between the process of ionization and the processes of the losses of charged particles. We do not take into account the recombination process. The ions disappear from the negative glow plasma due to their outflow to the cathode. The ions move in a collisionless regime under a potential difference  $kT_e/2e$ , which is applied to the so-called pre-sheath layer. Since the recombination losses are negligibly small and  $l_c \ll D/2$ , a length of the pre-sheath layer corresponds to  $D/2$ .

Total discharge current at the cathode surface  $i$  is a sum of the emission current  $i_{em}$  and the current of ions to the cathode  $i_i$ . The discharge current to anode is provided by the fast electrons from plasma that are able to overcome the potential barrier  $\Delta V$  near the anode.

In the generally accepted models, the ion emission current at the cathode surface is provided by the classical  $\gamma$  processes ( $i_{em} = \gamma i_i$ ) [9]. In our model we introduce the additional emission current at the cathode which appears due to a source of external emission  $i_{ext}$  [5]. It should be stressed that an external emission current is inevitably available in any type of glow discharge. For example, the negative glow plasma has to be considered as the external source of radiation with respect to the

cathode surface [10]. Then the component of external emission current is provided due to photoeffect at the cathode.

Beside that, there is a great variety of the discharges in which the other physical reasons for appearing the external current exist. The widespread reason for arising the current  $i_{ext}$  is formation of the spark cathode spots as a result of explosive processes at the cathode [2, 5, 11–14]. In the sources of electron and ion beams with plasma cathode [15–17], the additional emission current is often provided due to external injection of electrons in the plasma of hollow cathode or hollow anode. As for the particular case of this experiment, the high-emissivity tablet is responsible for the external emission current.

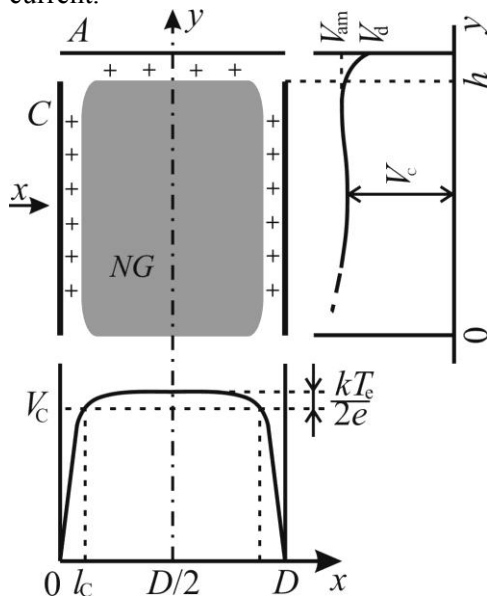


**Figure 4.** Schematic illustration of the discharge regions and the potential distributions as applied to the model of current sustaining in hollow cathode glow discharge.

*NG* – plasma of the hollow cathode (negative glow plasma);  $l_c$  – cathode voltage drop region;  $\Delta V = (V_{am} - V_d)$  – negative potential barrier near the anode;  $i = (i_{em} + i_i)$  – total discharge current at the cathode surface that is equal to current at the anode surface and in the external circuit.

Then in terms of the model, the emission current from the cathode can be written as

$$i_{em} = i_{ext} + \gamma i_i = i_i \left( \gamma + \frac{i_{ext}}{i_i} \right). \quad (1)$$

It is convenient to use an external parameter  $\delta$  as a fraction of the external emission current in the emission current appearing due to ion bombardment of the cathode

$$\delta = \frac{i_{ext}}{\gamma i_i}. \quad (2)$$

Equations (1) and (2) allow us to introduce a generalized coefficient of the secondary processes  $\Gamma$

$$\Gamma = \gamma + \frac{i_{ext}}{i_i} = \gamma \left( 1 + \frac{i_{ext}}{\gamma i_i} \right) = \gamma (1 + \delta). \quad (3)$$

After simple manipulations we can obtain the expression for total discharge current

$$i = i_c = i_a = i_{em} + i_i = (1 + \Gamma) i_i = \frac{1 + \Gamma}{\Gamma} i_{em}. \quad (4)$$

Proceeding from the power balance in the hollow cathode the condition for discharge sustaining can be obtained [5]

$$\Gamma \frac{V_c}{V_2} K_S = 1, \quad (5)$$

where  $K_S = (1 - S_D/S_C)$  is a geometrical factor ( $S_D$  – anode area,  $S_C$  – area of the surface of cathode cavity) and

$$V_2 = V^* + \frac{2kT_e}{e} + \Delta V + \Gamma \left( \frac{3kT_e}{2e} + \Delta V \right). \quad (6)$$

The physical meaning of  $V_2$  is the total cost of ionization under the effect of electron beam and  $V^*$  is the energy which the accelerated electron spends for one act of ionization with taking into account only the energy losses for gas excitation and for elastic collisions.

As distinct to [9], in the framework of this model, we can obtain a correlation between the total discharge current and the external emission current as

$$i_c = i_{ext} \left( 1 + \frac{1+\gamma}{\gamma\delta} \right) = i_{ext} \left( 1 + \frac{1+\gamma}{\Gamma-\gamma} \right) = i_{ext} K. \quad (7)$$

The results of estimations are presented in the Table below. In the calculations we have used the following parameters of the discharge:  $eV^* = 55$  eV,  $kT_e = 5$  eV,  $K_S \approx 1$ ,  $\Delta V \approx 0$ ,  $V_c = V_d$  [5]

**Table 1.** The results of estimates as applied to data presented in figures 2 and 3. The first line shows the operating points of the current-voltage characteristics.

	2	3	4	6
$V_d$ , V	398	416	396	127
$i$ , mA	16.6	24.5	25.5	16.3
$\Gamma$	0.166	0.159	0.167	0.544
$\delta$	0.387	0.326	0.394	3.533
$K = i/i_{ext}$	25.11	29.63	24.67	3.64
$l_c$ , cm	0.863	0.732	0.694	0.425

The point 1 is not suitable for estimation since the cathode layer length  $l_c$  is comparable with  $D/2$ . Minimal value of  $\Gamma = 0.159$  corresponds to point 3 of the hampered glow discharge. From this point a sharp transition to the regime II occurs. This transition is accompanied by a slight increase in generalized coefficient of secondary electron emission  $\Gamma$ . We believe that this increase is associated with the fact that the contribution of external current to emission current slightly increases.

The largest contribution of external current to total discharge current is observed in the case when high emissivity tablet is available in the cathode cavity. These conditions correspond to point 6 of current-voltage characteristic. Discharge burning voltage in this case is much less than for the regime II in figure 2, and coefficient  $\Gamma$  is three times higher.

The ratio of the external current to the current due to the ion bombardment is characterized by the parameter  $\delta = i_{ext}/\gamma i_i$ . To estimate this parameter we have to know the classical coefficient of secondary emission  $\gamma$ . In the calculations we use  $\gamma = 0.12$  [5]. Then for the case of the cathode with the high-emissivity tablet we obtain  $\delta = 3.53$ . It means that the current of external emission is more than three times higher as compared to the current due to ion bombardment of the cathode surface.

For the ordinary glow discharge with a hollow cathode a fraction of external current in total emission current  $i_{em}$  is small. Nevertheless, for the cases when emission current is set artificially, the contribution of the external current to the total emission current increases. For example, the balance of the currents at the cathode for the point 6 at figure 3 looks like as follows:  $i_i = 10.56$  mA,  $i_{ext} = 4.478$  mA,  $\gamma i_i = 1.32$  mA. Although the ion current is still higher than the emission current, this excess is not so considerable as for the classical glow discharge. This conclusion is illustrated by the estimation of

the coefficient  $K$ . For the hampered glow discharge, the typical values of the current enhancement coefficient is higher than 20. For the case of the cathode with the high emissivity, we obtain  $K \approx 3.5$ .

### Acknowledgments

The work was supported by Russian Science Foundation under the Grant # 14-19-00139.

### References

- [1] Frank K and Christiansen J 1989 The fundamentals of the pseudospark and its applications *IEEE Trans. Plasma Sci.* **17** 748-53
- [2] Korolev Y D and Frank K 1999 Discharge formation processes and glow-to-arc transition in pseudospark switch *IEEE Trans. Plasma Sci.* **27** 1525–37
- [3] Bochkov V D, Dyagilev V M, Ushich V G, Frants O B, Korolev Y D, Shemyakin I A and Frank K 2001 Sealed-off pseudospark switches for pulsed power applications (current status and prospects) *IEEE Trans. Plasma Sci.* **29** 802–8
- [4] Kozyrev A V, Korolev Y D, Rabotkin V G and Shemyakin I A 1993 Processes in the prebreakdown stage of a low-pressure discharge and the mechanism of discharge initiation in pseudospark switches *J. Appl. Phys.* **74** 5366–71.
- [5] Korolev Y D, Frants O B, Landl N V, Shemyakin I A and Geyman V G 2013 High-current stages in a low-pressure glow discharge with hollow cathode *IEEE Trans. Plasma Sci.* **41** 2087–96
- [6] Bochkov V D, Kolesnikov A V, Korolev Y D, Rabotkin V G, Frants O B and Shemyakin I A 1995 Investigation of the effect of blocking potential on the static breakdown voltage and discharge initiation in the pseudospark switches *IEEE Trans. Plasma Sci.* **23** 341–6
- [7] Meena B L, Rai S K, Tyagi M S, Pal U N, Kumar M and Sharma A K 2010 Characterization of high power pseudospark plasma switch (PSS) *J. Phys. Conference Series* **208** 012110
- [8] Zhang J, Zhao J P and Zhang Q G 2014 The breakdown characteristics of single-gap pseudospark discharge under nanosecond pulsed voltages *IEEE Trans. Plasma Sci.* **42** 2037–41
- [9] Ul'yanov K N 1999 Superdense glow discharge: Theoretical model of the cathode region *High Temperature* **37** 337–47
- [10] Kozhevnikov V Y, Kozyrev A V and Korolev Y D 2006 Drift model of the cathode region of a glow discharge *Plasma Phys. Reports* **32** 949–59
- [11] Kondrat'eva N P, Koval N N, Korolev Y D et al 1999 A spectroscopic investigation of the near-cathode regions in a low-pressure arc *J. Phys. D: Appl. Phys.* **32** 699–705
- [12] Korolev Y D, Frants O B, Geyman V G, et al 2012 Transient processes during formation of a steady-state glow discharge in air *IEEE Trans. Plasma Sci.*, **40** 2951–60
- [13] Korolev Y D, Frants O B, Landl N V, Bolotov A V and Nekhoroshev V O 2014 Features of a near-cathode region in a gliding arc discharge in air flow *Plasma Sources Sci. Technol.* **23** 054016
- [14] Korolev Y D, Frants O B, Landl N V, Kasyanov V S, Galanov S I, Sidorova O I, Kim Y, Rosocha L A and Matveev I B 2012 Propane oxidation in a plasma torch of a low-current nonsteady-state plasmatron *IEEE Trans. Plasma Sci.* **40** 535–42
- [15] Lopatin I V, Schanin P M, Akhmadeev Y H, Kovalsky S S and Koval N N 2012 Self-sustained low pressure glow discharge with a hollow cathode at currents of tens of amperes *Plasma Physics Reports* **38** 583–89
- [16] Ryabchikov A I, Arsubov N M, Vasilyev N A and Dektyarev S V 1991 The Raduga multipurpose ion source for surface modification of constructed materials *Nuclear Instruments Methods in Phys. Research Sect. B* **59** 124–7
- [17] Ryabchikov A I, Ryabchikov I A, Stepanov I B and Usov U P 2007 High-frequency short-pulsed metal plasma-immersion ion implantation or deposition using filtered DC vacuum-arc plasma *Surface Coatings Technology* **201** 6523–25